

Brassinosteroids control gravitropism by changing cellulose orientation and mannan content in Arabidopsis hypocotyls

Marc Somssich^a, Filip Vandenbussche^b, Alexander Ivakov^{c,1}, Norma Funke^{c,2}, Colin Ruprecht^{c,3}, Kris Vissenberg^{d,e}, Dominique Van Der Straeten^b, Staffan Persson^{a,4,5}, Dmitry Suslov^{f,4,5}

^a School of Biosciences, University of Melbourne, Parkville, VIC 3010, Melbourne, Australia; marc.somssich@unimelb.edu.au; staffan.persson@unimelb.edu.au

^b Laboratory of Functional Plant Biology, Ghent University, K.L. Ledeganckstraat 35, B-9000 Gent, Belgium; Filip.Vandenbussche@ugent.be; Dominique.VanDerStraeten@ugent.be

^c Max-Planck Institute of Molecular Plant Physiology, Am Muehlenberg 1, 14476 Potsdam, Germany

^d Biology Department, Integrated Molecular Plant Physiology Research, University of Antwerp, 2020 Antwerpen, Belgium; kris.vissenberg@uantwerpen.be

^e UASC-TEI, Plant Biochemistry and Biotechnology Lab, Department of Agriculture, School of Agriculture, Food, and Nutrition, Stavromenos, 71 004 Heraklion, Crete, Greece

^f Saint Petersburg State University, Faculty of Biology, Department of Plant Physiology and Biochemistry, 199034 Universitetskaya emb. 7/9, Saint Petersburg, Russia; d.suslov@spbu.ru

¹ Current address: Australian Institute of Sport, Leverrier st, Bruce, ACT, 2617, Australia

² Current address: Targenomix GmbH, Am Muehlenberg 11, 14476 Potsdam, Germany

³ Current address: Max-Planck Institute of Colloids and Interfaces, Am Muehlenberg 1, 14476 Potsdam, Germany

⁴ Co-senior authors.

⁵ Co-corresponding authors:

Dmitry Suslov

Saint Petersburg State University,

Faculty of Biology, Department of Plant Physiology and Biochemistry,

199034 Universitetskaya emb. 7/9, Saint Petersburg,

Russia

Email: d.suslov@spbu.ru

Staffan Persson

School of Biosciences, University of Melbourne,

36 Parkville, VIC 3010, Melbourne,
 37 Australia
 38 Email: staffan.persson@unimelb.edu.au
 39
 40 Date of submission: 10 December 2018
 41 Figures: 2 black and white; 5 in color (in print and online)
 42 Tables: 2
 43 Supplementary data: 1 figure, 10 videos
 44 Word count: 6444
 45

46 **Title:**

47 Brassinosteroids control gravitropism by changing cellulose orientation and mannan
48 content in Arabidopsis hypocotyls

49

50

51 **Running title:**

52 Cell wall polymers control shoot gravitropism

53

54 **Highlight**

55 Our data reveal new functions of cell wall polymers in gravitropic responses.
56 Brassinosteroid-related changes in shoot gravitropism uncover that cellulose re-
57 organization and mannan content influence shoot mechanical strength and bending.

58

59 **Abstract**

60 Shoot gravitropism is essential for plants to direct the growth of above-ground tissues
61 towards the soil surface after germination. Brassinosteroids influence shoot gravitropism
62 and we used this as a tool to untangle the function of cell wall polymers during etiolated
63 shoot growth. The ability of etiolated Arabidopsis seedlings to grow upwards was
64 suppressed in the presence of 24-epibrassinolide (EBL) but enhanced in the presence of
65 Brassinazole (BRZ), an inhibitor of brassinosteroid biosynthesis. These effects were
66 accompanied by changes in cell wall mechanics and composition. Cell wall biochemical
67 analyses and confocal microscopy of the cellulose-specific pontamine S4B dye revealed
68 that the EBL and BRZ treatments correlated with changes in cellulose fibre organization
69 and mannan content. Indeed, a longitudinal re-orientation of cellulose fibres supported
70 upright growth whereas the presence of mannans reduced gravitropic bending. The
71 negative effect of mannans on gravitropic bending is a new function for this class of
72 hemicelluloses, and provides insight into evolutionary adaptations by which aquatic
73 ancestors of terrestrial plants colonized land.

74

75 **Key words:** Arabidopsis, brassinosteroids, cellulose, cell wall, creep, evolution,
76 gravitropism, hypocotyl, mannan, shoot

77

78 Introduction

79 All growing plant cells are encased in primary cell walls, which are strong to maintain cell
80 and tissue integrity, yet extensible to allow for growth (Cosgrove, 2016). How these
81 conflicting properties are achieved is uncertain because the exact architecture of primary
82 cell walls is not well defined (Cosgrove, 2018). The traditional cell wall model, in which a
83 load-bearing network of cellulose microfibrils, cross-linked by hemicelluloses, is embedded
84 into an amorphous matrix of pectins and structural glycoproteins (Carpita and Gibeaut,
85 1993), has been substantially modified and improved (Cavalier *et al.*, 2008; Dick-Perez *et al.*,
86 2011). These modified models include a wall load-bearing capacity that is defined by
87 either lateral cellulose/xyloglucan/cellulose contacts in restricted areas called
88 “biomechanical hotspots” (Park and Cosgrove, 2012), and/or cellulose/pectin interactions
89 (Phyo *et al.*, 2017a, b), and/or arabinogalactan proteins covalently linked with pectin and
90 arabinoxylans (Tan *et al.*, 2013). At present, there is little consensus on the role of
91 particular polysaccharides in cell walls, and there is therefore a need for experimental
92 models that could help understand their functions and interactions. Negative gravitropism
93 of young plant shoots, i.e. their upright growth against the gravity vector, can be used as
94 one such model. Indeed, it is during this type of response that the conflicting properties of
95 growing walls are especially prominent: their extensibility should be delicately balanced
96 with the strength needed to maintain cell and tissue integrity, and to carry the weight of
97 upright shoots in the field of gravity. Hence, the effects of even moderate experimentally
98 imposed modifications of cell wall polymers could be revealed through changes in shoot
99 gravitropism. Negative shoot gravitropism also involves gravitropic bending, an
100 asymmetric shoot growth that restores its vertical position after inclination (Morita, 2010).
101 Studying this response can provide insight into compression resistance or the contribution
102 to plant organ flexibility of cell wall polymers, which is rarely addressed.

103 Brassinosteroids (BRs) constitute a class of phytohormones (Singh and Savaldi-
104 Goldstein, 2015) that impact the negative gravitropism of Arabidopsis hypocotyls, which is
105 largely supported by primary cell walls (Vandenbussche *et al.*, 2011). The gravitropic
106 response of hypocotyls was suppressed by epibrassinolide (EBL), one of the most active
107 natural BRs, while brassinazole (BRZ), a specific inhibitor of BR biosynthesis, stimulated it.
108 These effects did not result from modified gravity perception, but were accompanied by
109 changes in cell wall mechanics (Vandenbussche *et al.*, 2011). The biochemical basis of
110 the BR-induced alterations in wall physical properties is, however, largely unknown.
111 Comprehensive microarray data on BR effects on Arabidopsis plants revealed changes in
112 many dozens of cell wall-related genes (Goda *et al.*, 2002; Song *et al.*, 2009; Sun *et al.*,

2010; Yu *et al.*, 2011). Thus, the action of BRs, including that of EBL and BRZ, on Arabidopsis hypocotyl gravitropism could be mediated by a number of modifications at the cell wall level.

In the present work we combined high-resolution confocal microscopy, biochemical and biomechanical analyses of cell walls to study the mechanisms of EBL and BRZ action on the negative gravitropism of Arabidopsis hypocotyls.

Materials and methods

Plant material and growth conditions

Arabidopsis thaliana (L. Heynh.) wild type Columbia-0 and mutant plants were grown on half-strength Murashige and Skoog (MS) medium (pH 5.7) (Duchefa Biochemie) containing 0.68% (w/v) microagar (Duchefa Biochemie). Where indicated, the medium was supplemented with stock solutions of epibrassinolide (0.2 mM in methanol), brassinazole (2 mM in methanol) and oryzalin (500 μ M in ethanol), such that their final concentrations were 100 nM, 1 μ M and 250 nM, respectively. In each case the medium for control untreated plants was supplemented with corresponding volumes of methanol and/or ethanol.

Surface-sterilized seeds were sown aseptically on large (145×20 mm) round Petri plates (Greiner) containing the above-mentioned media. The seeds were stratified for 2 days at 4°C, and their synchronous germination was induced by exposure to fluorescent white light (150 μ mol m⁻² s⁻¹) for 6 h at 21°C. The moment of transfer to light, i.e. the beginning of induction, was taken as zero age for experimental plants. After the 6 h induction period the Petri plates were wrapped in two layers of thick aluminium foil and placed horizontally in an environmentally controlled growth room. Five-day-old etiolated plants grown at 21°C were used in experiments, unless specified otherwise.

Extensometry

Arabidopsis seedlings for creep tests were placed individually into 1.5 ml Eppendorf test tubes, frozen by plunging the closed tubes into liquid nitrogen, stored at -20°C and used for extensometry within two weeks after freezing. *In vitro* extension of frozen/thawed hypocotyls was measured with a custom-built constant load extensometer (Suslov and Verbelen, 2006). A 2- or 5-mm-long segment from the specified region of a hypocotyl was secured between clamps of the extensometer and preincubated in a buffer (20 mM MES-KOH, pH 6.0) in the relaxed state for 2 min. Then, its time-dependent extension (creep)

147 was measured in the same buffer under 625 mg or 750 mg loads for 15 min. The relative
148 creep rate was calculated as described in Vandenbussche *et al.* (2011).

149

150 *Cell wall biochemical analyses*

151 Approximately 300 of 5-day-old seedlings per sample were rapidly harvested to a large
152 volume of 70% EtOH, after which their seed coats were removed and discarded. The
153 resulting plant material was transferred to a 2 ml Eppendorf test tube, 1.5 ml of 70% EtOH
154 was added, followed by centrifugation at 10,000 rpm for 5 min discarding the supernatant.
155 One ml of acetone was added to the resulting pellet, followed by centrifugation at 10,000
156 rpm for 5 min. The supernatant was discarded, and the residue was air-dried overnight.
157 The resulting dry material was ball-milled (Retsch) for 1 min. One ml of EtOH was added
158 to the residue, followed by centrifugation at 21,000 g for 10 min discarding the
159 supernatant. Then 1 ml of MeOH:chloroform (1:1) mixture was added, followed by
160 centrifugation at 21,000 g for 10 min, discarding the supernatant and air-drying the pellet.
161 The resulting powdered cell wall pellet was weighed and transferred to a clean screw-
162 capped Eppendorf test tube. Myo-Inositol (30 μ l of 1 mg ml⁻¹ solution in water) was added
163 to the test tube as internal standard. Then 250 μ l of 2M TFA was added, followed by
164 incubation at 121°C for 1 h to hydrolyze cell wall polysaccharides. The tube was rapidly
165 cooled on ice, 300 μ l of 2-propanol was added and evaporated at 40°C, and the step with
166 2-propanol was repeated two more times. After this 250 μ l of H₂O was added, and the tube
167 was vortexed, sonicated for 10 min and centrifuged at 21,000 g for 10 min. One part of the
168 resulting supernatant was taken for uronic acids quantification (2 \times 50 μ l), and the other
169 portion (100 μ l) was dried and used for assaying cell wall monosaccharides, while the
170 pellet was processed for crystalline cellulose quantification. Subsequent cell wall
171 biochemical analyses were carried out as described in Sanchez-Rodriguez *et al.* (2012).
172 Uronic acids were colorimetrically measured using 2-hydroxydiphenyl as reagent (Vilím,
173 1985) with galacturonic acid as standard (Filisetti-Cozzi and Carpita, 1991). Cell wall
174 monosaccharides were assayed as alditol acetate derivatives (Neumetzler, 2010) using a
175 modified protocol from Albersheim *et al.* (1967) by gas chromatography performed on an
176 Agilent 6890N GC system coupled with an Agilent 5973N mass selective detector.
177 Crystalline cellulose was determined by Seaman hydrolysis (Selvendran and O'Neill,
178 1987) using Glc equivalents as standard, where the cellulosic Glc content was determined
179 with the anthrone assay (Dische, 1962).

180

181 *Microscopy*

Cellulose microfibrils were visualized in cell walls with Pontamine Fast Scarlet 4B (S4B) dye (Anderson *et al.*, 2010). In some experiments, living seedlings were stained in 0.2% (w/v) S4B for 30 min, which revealed microfibrils only in the upper growing parts of hypocotyls. To provide the dye penetration to the cell walls at the base of hypocotyls, plants were extracted under mild conditions by sequential washes with EtOH:100% acetic acid (7:1, v/v) for 1 h; 100% EtOH for 15 min; 50% EtOH in H₂O for 15 min; and 1M KOH in H₂O for 30 min. All washing steps were carried out on a rotator. Experimental samples were stored in 1M KOH at 4°C before analysis or used immediately after the last alkaline wash for cellulose visualization. The samples were rinsed in H₂O before staining to remove residual KOH, after which 0.2% (w/v) S4B was added for 30 min. Then they were rapidly rinsed with a large volume of H₂O to remove excessive dye and observed under a spinning disc confocal microscope or super-resolution Airyscan confocal microscope (LSM880). The equipment for spinning disc confocal microscopy included a Nikon Ti-E inverted confocal microscope equipped with a CSU-X1 spinning disc head (Yokogawa, Japan), a 100x CFI Apo oil immersion TIRF objective (NA 1.49, Nikon, Japan), an evolve charge-coupled device camera (Photometrics Technology, USA), and a 1.2x lens between the spinning disc and camera. S4B was excited using a 561 nm laser (similar to Anderson *et al.*, 2010). Image acquisitions were performed using Metamorph software (Molecular Devices, USA) version 7.5. High-resolution imaging of cellulose microfibrils was performed on a Zeiss LSM880 microscope equipped with an AiryScan Unit (Huff, 2015). S4B was excited using a 514 nm Argon Laser through a 458/514 MBS and a 63x Plan-Apochromat oil objective with a numeric aperture of 1.4. The 514 laser was used as 535 nm was indicated as an optimal S4B excitation wavelength (Anderson *et al.*, 2010) and as these settings provided good images for analyses. Emission was detected using the 32 GaAsP PMT array AiryScan unit. For each 8-bit image, a Z-stack consisting of 2-5 images with a 1 µm step-size, an image size of 1672x1672 pixels, and with 1.26 µs pixel dwell time was recorded. The recordings were deconvoluted using the Zeiss ZEN software at highest possible resolution.

Epidermal cell images at the base of hypocotyls were captured with a Leica DM 4000 light microscope equipped with a 1.3 megapixel CCD camera using a dark field mode, under a HCX PL FLUOTAR 20x/0.40 CORR objective. Cell lengths were then measured on digital images using a segmented line tool in ImageJ 1.49b software.

Time lapse photography by infrared imaging

For gravitropic reorientation assays, plants were grown in infrared light (930 nm) on vertical plates containing media. Plates with three-day-old seedlings were rotated 90° (time point 0). Subsequently, the seedlings were imaged using infrared enabled cameras (Vandenbussche *et al.*, 2010). Images were analysed using the angle tool in ImageJ.

Results

Brassinosteroids strongly affect etiolated shoot gravitropism in Arabidopsis

To corroborate that the gravitropic response of etiolated Arabidopsis seedlings was altered upon changes in BR signaling (Vandenbussche *et al.*, 2011), we grew seedlings on horizontal Petri plates in the presence of exogenous EBL or BRZ and counted upright hypocotyls (Fig. 1). Plants grown on one-half strength MS media had 40-80% of upright hypocotyls (Fig. 1A). Media supplemented with EBL (100 nM) resulted in a decreased proportion of standing hypocotyls to 0-5% (Fig. 1B), while media containing BRZ (1 µM) increased it to 90-100% (Fig. 1C). These observations were consistent essentially from the moment of germination and demonstrate that BRs negatively affect shoot gravitropism.

Brassinosteroids influence etiolated shoot gravitropism via changes in cell wall mechanics

The influence of EBL on gravitropism (Fig. 1B) was hypothesized to emanate from cell wall weakening and thus an inability to keep hypocotyls upright in the field of gravity (Vandenbussche *et al.*, 2011). EBL had no effect on gravitropic bending in Arabidopsis plants grown on vertical Petri plates and gravistimulated by a 90 degrees clockwise rotation of the plates (see Fig. 4 in Vandenbussche *et al.*, 2011). In contrast, BRZ increased both the percentage of upright hypocotyls and their gravitropic bending, but its effect on cell wall mechanics remains unclear (Vandenbussche *et al.*, 2011).

We used the creep (constant-load) method to assess the biomechanical control of shoot gravitropism. Whenever hypocotyl length afforded, we stretched their basal regions, carrying the main part of the organ weight in the field of gravity, as well as their apical growing regions that are responsible for gravitropic bending (Fig. 2A). The scheme in Figure 2A illustrates the established age-dependent shift of growth zones in etiolated Arabidopsis hypocotyls; from the base towards cotyledons (Gendreau *et al.*, 1997; Bastien *et al.*, 2016). As BRZ greatly inhibited etiolated hypocotyl elongation (Fig. 1A, C), we compared cell wall creep in BRZ-grown plants with their age-matched 6-day-old untreated counterparts, as well as with 3-day-old untreated “genetic controls”, which are approximately the same length as the 6-day-old BRZ-grown plants (Fig. 2B). BRZ significantly decreased creep rates compared with both controls, which is consistent with

cell wall strengthening. Thus, the inhibition of BR biosynthesis leads to an increase in negative gravitropism of hypocotyls, not only through the stimulation of gravitropic bending (Fig. 4 in Vandenbussche *et al.*, 2011), but also by cell wall strengthening that confers support to hypocotyls in the field of gravity (Fig. 2B). The creep rate analyses in EBL-grown plants revealed that the weakening of cell walls was mostly restricted to the basal nonexpanding hypocotyl zones (Fig. 2C-E). Hence, EBL may affect gravitropism (Fig. 1B) by interfering with the cell wall strengthening, which takes place in the basal regions of etiolated hypocotyls (Fig. 2D, E) where cell expansion has already ceased (Gendreau *et al.*, 1997).

260

261 *Changes in cell wall biochemistry underpin the effects of BRs on gravitropism*

262 To investigate how the cell walls are altered during BR exposure, thereby influencing cell
263 wall mechanics and hypocotyl gravitropism, we performed standard cell wall biochemical
264 analyses (Fig. 3). The content of uronic acids, which are the principal constituents of
265 pectins, was unaffected by the EBL or BRZ treatments (Fig. 3A). By contrast, crystalline
266 cellulose levels were significantly decreased in BRZ treated seedlings as compared with
267 the untreated control, while EBL had no effect on this polymer level (Fig. 3B). As for
268 monosaccharide composition of cell wall matrix polymers, both EBL and BRZ treatments
269 significantly increased rhamnose content (Fig. 3C). In addition, BRZ treatment decreased
270 mannose and increased glucose in cell wall matrix polysaccharides (Fig. 3C). Changes in
271 rhamnose are likely due to the metabolism of rhamnogalacturonan I, which is the main
272 source of this monosaccharide in primary cell walls. As EBL and BRZ caused opposite
273 effects on gravitropism (Fig. 1B, C) but induced very similar increases in rhamnose (Fig.
274 3C), we argued that it is unlikely that this sugar is underpinning our observed phenotype.
275 We did therefore not consider the rhamnose change in further details. Mannose is the
276 principal constituent of cell wall mannans and the BRZ-induced decrease of mannose
277 could therefore be caused by partial mannan depletion in the seedling cell walls. The BRZ-
278 induced increase in glucose was not accompanied by any xylose accumulation (Fig. 3C)
279 indicating that it is not associated with xyloglucans. On the other hand, the increase in
280 glucose correlated with a decrease in crystalline cellulose (Fig. 3B). The inverse
281 relationship between crystalline cellulose (Fig. 3B) and glucose (Fig. 3C) could be
282 explained by a larger amorphous component of cellulose microfibrils, which is likely to be
283 sensitive to TFA hydrolysis, perhaps explaining the apparent increase in glucose content
284 in BRZ treated seedlings (Fig. 3C).

285

EBL-induced suppression of etiolated hypocotyl gravitropism is related to cellulose arrangement

Rather unexpectedly, the strong effect of EBL on cell wall mechanics (Fig. 2C-E) was not associated with prominent changes in cell wall biochemical composition (Fig. 3). Nevertheless, not only the levels of certain cell wall polymers, but also their orientations and interactions in the wall affect cell wall mechanics, with implications both on cellular strength and expansion. This is especially true for cellulose, the strongest cell wall component (Suslov and Verbelen, 2006; Suslov *et al.*, 2009). To examine the orientation of cellulose in outer epidermal cell walls of hypocotyls from control and EBL-grown plants we used the specific fluorescent dye Pontamine Fast Scarlet 4B (S4B) (Anderson *et al.*, 2009). We imaged the dye-associated cellulose fibers using spinning-disc or high-resolution Airyscan confocal microscopy. With these set-ups we could reveal distinct cellulose macrofibril orientations. To improve the penetration of the dye and visualization of the cellulose fibers along the whole hypocotyl length we performed a mild extraction of cell walls. Without this treatment the cellulose fibers were not well discerned in the basal parts of living hypocotyls. Nevertheless, we made sure that living and extracted seedlings displayed similar cellulose arrangements in the upper growing region of their hypocotyls. In this part of control seedlings transverse buckling was frequently observed in the innermost wall layer. This phenomenon occurred in approximately 50% of both living and extracted control hypocotyls, and complicated cellulose macrofibril visualization on the inner wall face. In the remaining samples, i.e. in which we did not observe the buckling, cellulose macrofibrils were clearly transverse in the innermost wall layer and longitudinal in the outermost layer (Supplementary Video S1; Fig. 4A; Table 1). In the basal non-growing region of control hypocotyls, we observed slight or no buckling of the wall inner surface. These walls contained less transverse macrofibrils in the innermost layer and more thick longitudinal macrofibrils in the outermost layer compared with the upper growing region of hypocotyls (Supplementary Video S2; Fig. 4D; Table 1). In the upper region of approximately 50% of hypocotyls from EBL-grown plants, we observed irregular buckling in the innermost wall. In the samples without buckling, cellulose macrofibrils were more obliquely oriented (Fig. 4B), or decreased in relative abundance, compared with the untreated control. EBL did not influence longitudinal macrofibrils in the outermost wall layer in the growing zone of hypocotyls (Supplementary Video S3). The most dramatic EBL effect on cellulose orientation was found in the basal region of hypocotyls where it essentially eliminated longitudinal macrofibrils, such that the remaining ones were apparently thinner and had either oblique or random orientation (Fig. 4E; Supplementary

321 Video S4; Table 1). This reduction in longitudinal macrofibrils at the hypocotyl base was a
322 unique effect observed only in EBL-treated seedlings (Table 1; Fig. 4).

323 To confirm that the EBL-induced suppression of gravitropism was associated with
324 macrofibril disorganization, we attempted to “randomize” cellulose orientation in the cell
325 walls and then see how this affected the percentage of standing hypocotyls (Fig. 5). For
326 this purpose, Arabidopsis seedlings were grown in the presence of 250 nM oryzalin, which
327 partially disassembles cortical microtubules, thereby affecting the direction of cellulose
328 microfibril deposition in the cell wall (Paredes *et al.*, 2006). This low concentration of
329 oryzalin induced similar changes in cellulose arrangement as those observed with EBL in
330 the upper part of hypocotyls (compare Supplementary Video S5 with Supplementary Video
331 S3; Fig. 4B, G; Table 1), and significantly decreased the percentage of standing
332 hypocotyls (Fig. 5). Thus, intact cellulose orientation is important for the negative
333 gravitropism of hypocotyls, and the mechanism of EBL action on gravitropism may be
334 based on changes in cellulose arrangement. However, the effect of oryzalin on the
335 percentage of upright hypocotyls (Fig. 5) was weaker than that of EBL (Fig. 1B). This
336 difference can be explained by the inability of oryzalin to alter longitudinal cellulose
337 macrofibrils in the basal region of hypocotyls, in contrast to the effect of EBL (compare
338 Supplementary Video S6 with Supplementary Video S4; and Fig. 4E with Fig. 4I; Table 1).
339 These longitudinal macrofibrils accumulated in the outermost wall layer where they appear
340 to contribute to the mechanical strength and upright growth of hypocotyls. Their reduced
341 presence in EBL-treated seedlings (Fig. 4E, Supplementary Video S4) correlated with
342 weaker walls at the base of hypocotyls (Fig. 2D, E).

343

344 *BRZ increases the negative gravitropism of etiolated hypocotyls via several different*
345 *mechanisms*

346 Interestingly, the promoting effect of BRZ on gravitropism was independent of oryzalin
347 treatment (250 nM) (Fig. 5). These data suggest that BRZ either regulates gravitropism
348 somewhat independently of cellulose orientation, and/or antagonizes the oryzalin-induced
349 macrofibril randomization. Our microscopic observations supported the first option,
350 because we observed less ordered cellulose orientations in the upper parts of seedlings
351 treated with oryzalin and BRZ (Fig. 4C, H; Supplementary Videos S7, S8; Table 1). At the
352 same time the cellulose arrangement in the basal hypocotyl part was essentially similar in
353 the untreated controls and seedlings grown in the presence of BRZ, oryzalin, and BRZ
354 plus oryzalin (Fig. 4D, F, I, J; Supplementary Videos S2, S6, S9, S10; Table 1).

Our cell wall biochemical data suggest that BRZ may affect gravitropism in a cellulose-independent manner. One such mechanism might be mediated by reducing the mannan content (Fig. 3C). To assess whether a decrease in mannan content affected negative gravitropism we studied triple *cs/a2cs/a3cs/a9* mutant plants lacking detectable glucomannans (Goubet *et al.*, 2009). The triple mutation did not influence the percentage of standing hypocotyls (Supplementary Fig. S1). However, by analogy with BRZ, the mutants displayed significantly accelerated gravitropic bending in reorientation assays with plants grown on vertical Petri plates (Fig. 6). Interestingly, the coefficient of BRZ stimulation of gravitropic bending was reduced in the background of *cs/a2cs/a3cs/a9* compared with Col-0 (Fig. 6, Table 2). The above findings show that the decreased mannan content (Fig. 3C) accounts – at least in part - for the BRZ-induced increase in gravitropic bending.

Plant cell expansion is known to be induced by cell wall loosening (Cosgrove, 2016; Ivakov *et al.*, 2017). Cell growth is slow and uniform along the length of young etiolated hypocotyls that have just emerged from germinating seeds (Refrégier *et al.*, 2004). A wave of rapid cell expansion starts at the base of hypocotyls at about 48 h post induction, after which it spreads acropetally towards cotyledons (Gendreau *et al.*, 1997; Bastien *et al.*, 2016). Hence, cell wall loosening is highly induced in the basal region of hypocotyls carrying their whole weight, which can interfere with keeping the upright position of this organ in the field of gravity. As the effect of BRZ on gravitropism is seen from the moment of hypocotyl emergence from seeds, it can result, among other things, from the particular distribution of cell expansion and, hence, cell wall loosening in very young hypocotyls. To test this option, cell length was measured in epidermal cell files at two developmental stages (Fig. 7A), allowing growth rate calculation for individual cells along hypocotyls (Fig. 7B). Only lower halves of epidermal cell files comprising ten cells were considered. These are the regions where the rapid growth is first initiated in hypocotyls (Gendreau *et al.*, 1997). Cell length was measured at 55 h post induction, the time point corresponding to the earliest phase of rapid growth in hypocotyls (Pelletier *et al.*, 2010), and at 72 h post induction, when maximal growth rate is attained (Gendreau *et al.*, 1997). Epidermal cell length was significantly lower in hypocotyls of BRZ-treated vs. control plants for all cells with the exception of the first cell at 55 h illustrating severe growth inhibition due to a decrease in BRs biosynthesis (Fig. 7A). The rate of cell expansion was also significantly lower for the majority of cells in BRZ-treated vs. control plants suggesting that the wall loosening was inhibited in the former (Fig. 7B). Interestingly, two peaks of growth inhibition were observed in BRZ-treated seedlings: at the base of hypocotyls (cells one and three)

and in their most apical zone examined (cells nine and ten) (Fig. 7B). Thus, the wave of rapid growth is initiated in a higher region of hypocotyls and spreads acropetally slower in BRZ-treated vs. control plants. Overall, the above data suggest that cell wall loosening is inhibited more strongly at the base of hypocotyls, i.e. in the region responsible for carrying the seedling weight in the field of gravity. This inhibition can be another mechanism by which BRZ increases the percentage of standing hypocotyls.

Discussion

The two prerequisites for normal negative gravitropism in young shoots, mechanical strength and gravitropic bending, are based on distinct physiological mechanisms, which are linked through the cell wall characteristics. The mechanical strength of young shoots is defined by turgor and their primary cell walls (Shah *et al.*, 2017). This is well illustrated by wilting, a loss of turgor, when young shoots do not keep their upright position and lie down on the ground. Turgor depends on the transmembrane concentration gradient of osmotically active compounds, the hydraulic conductance and wall yielding properties (Ray *et al.*, 1972). It is said to be in dynamic balance between wall yielding, which tends to decrease turgor, and water uptake, which tends to increase turgor pressure (Cosgrove, 1986). Hence, changes in the wall properties, reflected by increasing (Fig. 2C-E) and decreasing (Fig. 2B) creep rates in the presence of EBL and BRZ, respectively, will contribute to lower and higher turgor values, which underpin the BR effect on gravitropism (Fig. 1). However, we cannot exclude that these effects are partially mediated by osmotic adjustments also influencing turgor pressure, which was not addressed here. Similarly, the selective BRZ-induced growth inhibition at the hypocotyl base (Fig. 7B), presumably mediated by decreased cell wall yielding, could elevate turgor, thereby maintaining their upright position.

Gravitropic bending results from asymmetric cell expansion on the opposite flanks of gravistimulated organs (Millner *et al.*, 2007). In young shoots put horizontally this response originates from simultaneous growth inhibition and stimulation on their upper and lower flanks, respectively (Bagshaw and Cleland, 1990; Cosgrove, 1990a; Ikushima *et al.*, 2008). As in the case of cell expansion in vertical plant organs (Cosgrove, 2018), the growth responses during gravitropic bending are controlled by cell wall yielding properties (Bagshaw and Cleland, 1990; Cosgrove, 1990b; Edelmann and Samajova, 1999; Ikushima *et al.*, 2008). Cell wall extensibility always decreases on the upper sides and sometimes increases on the lower sides of gravistimulated shoots, such that the overall cell wall loosening or tightening prevails depending on the species (Edelmann, 1997) and/or the

425 phase of gravitropic bending (Bagshaw and Cleland, 1990). However, this prevalent
426 overall loosening and tightening will not affect the percentage of standing 5- and 6-day old
427 *Arabidopsis* hypocotyls in which the zone of gravitropic bending is physically separated
428 from the basal zone that is mostly responsible for the mechanical strength needed for
429 shoot gravitropism (Fig. 2A).

430 There is another scenario in which gravitropic bending can contribute to the
431 percentage of standing young shoots. Seeds of plant species, which have no special
432 adaptive mechanisms for oriented dispersal on the soil surface, will land on it with random
433 orientations. Those seeds in which embryonal shoots are directed upwards in/on the soil
434 will have a higher chance to produce standing hypocotyls as this seed orientation
435 minimizes any contacts of growing shoots with the potentially adhesive soil surface. The
436 embryonal shoots of seeds oriented upside down in/on the soil will have to efficiently bend
437 to attain the correct upward orientation. It is hypothesized that the more rapid the shoot
438 bends, the lower its contacts with the adhesive surrounding soil, leading to a higher
439 percentage of standing shoots. In general, rapid growth is nonoptimal for negative
440 gravitropism in shoots because it decreases their mechanical strength. Hence, cell
441 extension should be very delicately controlled at the base and during bending of young
442 shoots to support their negative gravitropism.

443 Cellulose is the strongest cell wall component. The requirement of high wall
444 mechanical strength for shoot gravitropism suggests that the arrangement of microfibrils
445 could affect this process. The modulus of individual cellulose microfibrils ranges from 0.7
446 to 3.5 GPa (Chanliaud *et al.*, 2002), which is about 100-fold greater than the tensile
447 modulus of primary cell walls (Ryden *et al.*, 2003). Due to this fact, cellulose microfibrils
448 never extend axially under physiological conditions, instead they separate from each other,
449 bend, slide past each other and reorient in the direction of strain during growth, or under
450 external forces, resulting in cell wall deformations (Preston, 1982; Refrégier *et al.*, 2004;
451 Zhang *et al.*, 2017). The cellulose mobility depends on microfibril-microfibril and microfibril-
452 matrix interactions, proteinaceous cell wall loosening/tightening factors (Chanliaud *et al.*,
453 2002; Chanliaud *et al.*, 2004; Zhang *et al.*, 2017) and cellulose orientation that is defined
454 by cortical microtubules (Paredes *et al.*, 2006; Bringmann *et al.*, 2012). BRs affect many
455 processes linked with cellulose. They transcriptionally regulate the majority of *CESA* genes
456 encoding catalytic subunits of cellulose synthase complexes through the involvement of
457 the BR-activated transcription factor BES1 (Xie *et al.*, 2011). Additionally, BRs influence
458 cellulose synthesis posttranslationally: the negative regulator of BR signaling,
459 BRASSINOSTEROID INSENSITIVE2 (BIN2), can phosphorylate one of the cellulose

460 synthase subunits that leads to impaired cellulose synthesis (Sanchez-Rodriguez *et al.*,
461 2017). These mechanisms can be the cause for the BRZ-induced decrease in cellulose
462 content (Fig. 3B). BRs may also change microfibril orientation as they influence cortical
463 microtubule organization (Gupta *et al.*, 2012), possibly via BIN2 (Liu *et al.*, 2018). Hence,
464 the EBL-induced formation of oblique cellulose macrofibrils in the inner wall layer adjacent
465 to the plasma membrane (Fig. 4B, E; Table 1; Supplementary Movies S3 and S4) may
466 result from cortical microtubule reorientations.

467 We observed two additional cellulose-related effects of BRs. First, the BRZ-induced
468 decrease in crystalline cellulose and increase in the TFA-released glucose, without
469 increase in xylose (Fig. 3B, C), can be interpreted as a decrease in the cellulose
470 crystallinity. Similar observations were made in *isoxaben resistant (ixr)* mutants (DeBolt *et al.*,
471 2013). BRZ could thus generate cellulose microfibrils with reduced crystallinity and
472 more exposed glucan chains. This might provide a larger surface area, and thus additional
473 sites, for noncovalent interactions with adjacent microfibrils and matrix polysaccharides.
474 The 'rough' surface of such microfibrils could also provide a better access for enzymes
475 forming covalent cross-links between cell wall components. A good candidate for this role
476 is AtXTH3 that catalyses cellulose-cellulose, cellulose-xyloglucan and xyloglucan-
477 xyloglucan transglycosylation (Shinohara *et al.*, 2017). All these additional noncovalent
478 and covalent interactions could explain the increased wall mechanical strength observed
479 with BRZ treatment (Fig. 2B) that contributes to the negative gravitropism of hypocotyls
480 (Fig. 1C).

481 The second cellulose-related effect of BRs is the EBL-induced macrofibril
482 disorganization at the base of hypocotyls (Fig. 4E; Supplementary Video S4). The overall
483 arrangement of macrofibrils along Arabidopsis hypocotyls is consistent with the classical
484 multinet growth theory, according to which cellulose is deposited transversely next to the
485 plasma membrane, followed by a passive microfibril displacement into deeper wall layers
486 and their axial reorientation, i.e. parallel to the direction of maximal growth (Roelofsen,
487 1958; Preston, 1982; Refrégier *et al.*, 2004). Transverse and longitudinal macrofibrils were
488 observed in the inner and the outer wall layer, respectively, both in the upper and the lower
489 half of control hypocotyls (Supplementary Videos S1 and S2). Longitudinal macrofibrils
490 were clearly more prevalent in the lower fully elongated region compared with the upper
491 elongating region of hypocotyls, because in the former zone they had more time for the
492 passive reorientation in the direction of growth. Cellulose in the upper half of EBL-treated
493 hypocotyls also demonstrated a multinet-like axial reorientation from rare oblique
494 macrofibrils in the inner wall layer to thick abundant longitudinal macrofibrils in its outer

layer (Supplementary Video S3). The lower halves of these hypocotyls contained relatively abundant oblique macrofibrils with few thin longitudinal macrofibrils on the outer wall face (Supplementary Video S4). Keeping in mind that epidermal cells at the base of hypocotyls are at a later developmental stage than those at the apex (Gendreau *et al.*, 1997; Bastien *et al.*, 2016), it means that the majority of longitudinal macrofibrils in the outer wall layer are post-synthetically re-oriented to produce oblique ones in fully elongated cells. A force that drives such re-orientation must be very high. The most likely candidate for this role is a change in the wall hydration generating forces that can rearrange cellulose microfibrils (Huang *et al.*, 2018). In line with this hypothesis BRs were shown to induce a rapid wall swelling (Caesar *et al.*, 2011). Irrespectively of the mechanisms involved, the elimination and thinning of longitudinal cellulose macrofibrils observed at the base of hypocotyls from EBL-grown plants could decrease their resistance to bending, such that they can easily curve under their own weight and fall on the agar surface (Fig. 1B), which would decrease the negative gravitropism of hypocotyls.

Mannans are minor hemicelluloses of primary cell walls in angiosperms. Their backbones are either composed of (1→4)-β-D-mannose residues only (pure mannan), or contain (1→4)-β-linked D-glucose and D-mannose residues distributed along the chain in a non-regular fashion (glucomannan). Both polysaccharides can have (1→6)-α-D-galactose substitutions on their backbones, in which case they are referred to as galactomannans and galactoglucomannans, respectively (Schröder *et al.*, 2009). Mannans are often utilized as storage polysaccharides in seeds, bulbs and tubers. They also seem to play a structural role in the secondary cell walls of gymnosperms, where mannans are abundant (Hosoo *et al.*, 2002), and such a role was inferred from the experiments on cell wall analogues (Whitney *et al.*, 1998). However, doubts have been cast on the structural functions of mannans in primary cell walls based on the phenotype of *Arabidopsis* triple mutant *cs/a2cs/a3cs/a9*. Being deficient in mannan biosynthesis and containing no detectable glucomannans, the mutant seedlings were phenotypically indistinguishable from their wild type counterparts (Goubet *et al.*, 2009). Our findings that BRZ decreases the content of mannose in cell wall matrix polysaccharides (Fig. 3C), while increasing the gravitropic bending of hypocotyls (Vandenbussche *et al.*, 2011; Fig. 6), and that the triple mutation *cs/a2cs/a3cs/a9* increases the gravitropic curvature (Fig. 6) with no effect on the percentage of upright hypocotyls (Supplementary Fig. S1) show that mannans have a negative effect on gravitropic bending. This role in shoot gravitropism is a new function for mannan polysaccharides. Interestingly, our data are consistent with the fact that gravistimulation of wild type *Arabidopsis* seedlings is accompanied by a strong

530 downregulation of one *CSLA* gene responsible for mannan biosynthesis (Millar and Kiss,
531 2013). Additionally, the level of galactoglucomannans was decreased by about 50% in
532 maize stem pulvini as a result of gravistimulation (Zhang *et al.*, 2011). The negative
533 influence of mannans on shoot gravitropism is interesting from an evolutionary
534 perspective. Aquatic ancestors of terrestrial plants used buoyancy to support their bodies
535 (Hejnowicz, 1997). Hence, the mechanisms of shoot gravitropism evolved when plants
536 began to thrive on land instead of in an aquatic environment. According to recent data,
537 terrestrial plants originated from the advanced charophycean green algae (CGA) of the
538 order Zygnematales (Wickett *et al.*, 2014). CGA cell walls contain mannans and xylans as
539 principal hemicelluloses (Popper and Tuohy, 2010), whereas xyloglucans emerge in some
540 members of this group including Zygnematales (Sørensen *et al.*, 2010). The evolution of
541 terrestrial plants involves a gradual increase in the xyloglucan content of primary cell walls
542 and an opposite trend for mannans (Popper, 2008). These data suggest that the
543 emergence of xyloglucans in CGA might have formed a basis for subsequent land
544 colonization. At the same time, the properties of mannans may not be well suited for land
545 habitats. In this evolutionary context it is important to find out why mannans interfere with
546 gravitropic bending. The precise mechanism of the effect is unknown, but we consider
547 three hypotheses:

548 1) Glucomannans have less regularly organized backbones than xyloglucans
549 (Schroder *et al.*, 2009) making them insufficiently flexible alone or in a complex with
550 different cell wall components to support the rapid formation of gravitropic bending.

551 2) Mannans could interfere with the activities of xyloglucan
552 endotransglucosylase/hydrolases (XTHs) that seem to participate in the mechanism of
553 gravitropic bending (Zhang *et al.*, 2011; Hu *et al.*, 2013). XTHs were shown to use non-
554 xyloglucan polysaccharides as donor substrates, although much less efficiently than
555 xyloglucans (Maris *et al.*, 2011; Shinohara *et al.*, 2017). If XTHs have some affinity for
556 mannans, their presence could decrease the enzyme's action on xyloglucans in a
557 competitive manner, thereby impairing the function of specific XTHs during gravitropism.

558 3) Changes in mannan synthesis can affect gravitropic bending by modulating the
559 level of reactive oxygen species (ROS). This scenario is possible because GDP-mannose
560 is a common precursor in the biosynthesis of mannans and ascorbate (Sawake *et al.*,
561 2015). Accordingly, the downregulation of *CSLA* gene expression by gravistimulation
562 (Millar and Kiss, 2013), BRZ or different cues will increase the GDP-mannose pool
563 available for ascorbate biosynthesis. The resulting increase in ascorbate, a strong

antioxidant, will modulate ROS levels, which are important for gravitropic responses (Joo *et al.*, 2001; Krieger *et al.*, 2016; Singh *et al.*, 2017; Zhou *et al.*, 2018).

These mechanisms are not mutually exclusive. Studying their contribution to shoot gravitropism will shed light to the role of mannans in cell wall architecture. This could also improve our understanding of key cell wall modifications that allowed successful land colonization by aquatic ancestors of terrestrial plants.

In summary, by studying the effects of brassinosteroids on shoot gravitropism at the cell wall level we have revealed that mannans interfere with gravitropic bending of *Arabidopsis* hypocotyls, which is a new function for these minor hemicelluloses of primary cell walls. Additionally, both the pattern of cellulose macrofibrils and slow cell expansion at the base of hypocotyls are important for their upright growth during negative gravitropism. Thus, the modulation of brassinosteroid content in shoot gravitropism studies provides a convenient system for revealing the functions of polymers in primary cell walls.

Supplementary data

Supplementary data are available at *JXB* online.

Figure S1. The percentage of standing hypocotyls in *Col-0* and *cs1a2cs1a3cs1a9* *Arabidopsis* seedlings.

Video S1. Cellulose macrofibrils in the upper region of hypocotyls from control seedlings. In this and following videos cellulose arrangement is represented in the order from the innermost to the outermost layer of the outer epidermal cell wall.

Video S2. Cellulose macrofibrils in the basal region of hypocotyls from control seedlings.

Video S3. Cellulose macrofibrils in the upper region of hypocotyls from EBL-grown seedlings.

Video S4. Cellulose macrofibrils in the basal region of hypocotyls from EBL-grown seedlings.

Video S5. Cellulose macrofibrils in the upper region of hypocotyls from oryzalin-grown seedlings.

Video S6. Cellulose macrofibrils in the basal region of hypocotyls from oryzalin-grown seedlings.

Video S7. Cellulose macrofibrils in the upper region of hypocotyls from BRZ-grown seedlings.

Video S8. Cellulose macrofibrils in the upper region of hypocotyls from seedlings grown with BRZ plus oryzalin.

598 **Video S9.** Cellulose microfibrils in the basal region of hypocotyls from BRZ-grown
599 seedlings.

600 **Video S10.** Cellulose microfibrils in the basal region of hypocotyls from seedlings grown
601 with BRZ plus oryzalin.

602

603 **Acknowledgements**

604 MS and SP would like to acknowledge the support from the Biological Optical Microscopy
605 Platform (BOMP) at the University of Melbourne. MS is funded through a postdoctoral
606 fellowship by the Deutsche Forschungsgemeinschaft (DFG) (Project 344523413). KV
607 acknowledges the University of Antwerp and the National Research Foundation (FWO-
608 Vlaanderen) for grants G.0.602.11.N.10 and G039815N. DVDS acknowledges the
609 Research Foundation Flanders (project G.0656.13N) and Ghent University for financial
610 support. SP was funded by an ARC future fellowship grant (FT160100218) and
611 acknowledges an UoM IRRTF (RNC) grant. DS acknowledges DAAD for the research
612 grants of “Dmitry Mendeleev” program in 2012 and 2014, RFBR for the grant No 15-04-
613 04075, Saint Petersburg State University for the grant 1.40.492.2017 and the Research
614 park of Saint Petersburg State University: Center for Molecular and Cell Technologies, and
615 Chromas Core Facility. We are grateful to Professor Paul Dupree (University of
616 Cambridge) for the kind gift of *cs/a2cs/a3cs/a9* seeds.

References

- Albersheim P, Nevins DJ, English PD, Karr A.** 1967. A method for the analysis of sugars in plant cell-wall polysaccharides by gas-liquid chromatography. *Acer pseudoplatanus* tissue culture cells. *Carbohydrate Research* **5**, 340–345.
- Anderson CT, Carroll A, Akhmetova L, Somerville C.** 2010. Real-time imaging of cellulose reorientation during cell wall expansion in *Arabidopsis* roots. *Plant Physiology* **152**, 787–796.
- Bagshaw SL, Cleland RE.** 1990. Wall extensibility and gravitropic curvature of sunflower hypocotyls: correlation between timing of curvature and changes in extensibility. *Plant Cell and Environment* **13**, 85–89.
- Bastien R, Legland D, Martin M, Fregosi L, Peaucelle A, Douady S, Moulia B, Höfte H.** 2016. KymoRod: a method for automated kinematic analysis of rod-shaped plant organs. *Plant Journal* **88**, 468–475.
- Bringmann M, Li E, Sampathkumar A, Kocabek T, Hauser MT, Persson S.** 2012. POM-POM2/cellulose synthase interacting1 is essential for the functional association of cellulose synthase and microtubules in *Arabidopsis*. *Plant Cell* **24**, 163–177.
- Caesar K, Elgass K, Chen Z, Huppenberger P, Witthöft J, Schleifenbaum F, Blatt MR, Oecking C, Harter K.** 2011. A fast brassinolide-regulated response pathway in the plasma membrane of *Arabidopsis thaliana*. *Plant Journal* **66**, 528–540.
- Carpita NC, Gibeaut DM.** 1993. Structural models of primary cell walls in flowering plants: consistency of molecular structure with the physical properties of the walls during growth. *Plant Journal* **3**, 1–30.
- Cavalier DM, Lerouxel O, Neumetzler L, et al.** 2008. Disrupting two *Arabidopsis thaliana* xylosyltransferase genes results in plants deficient in xyloglucan, a major primary cell wall component. *Plant Cell* **20**, 1519–1537.
- Chanliaud E, Burrows KM, Jeronimidis G, Gidley MJ.** 2002. Mechanical properties of primary plant cell wall analogues. *Planta* **215**, 989–996.
- Chanliaud E, De Silva J, Strongitharm B, Jeronimidis G, Gidley MJ.** 2004. Mechanical effects of plant cell wall enzymes on cellulose/xyloglucan composites. *Plant Journal* **38**, 27–37.
- Cosgrove D.** 1986. Biophysical control of plant cell growth. *Annual Review of Plant Physiology* **37**, 377–405.
- Cosgrove DJ.** 1990a. Rapid, bilateral changes in growth rate and curvature during gravitropism of cucumber hypocotyls: implications for mechanism of growth control. *Plant Cell and Environment* **13**, 227–234.
- Cosgrove DJ.** 1990b. Gravitropism of cucumber hypocotyls: biophysical mechanism of altered growth. *Plant Cell and Environment* **13**, 235–241.

Cosgrove DJ. 2016. Catalysts of plant cell wall loosening [version 1; referees: 2 approved]. *F1000Research* **5**(F1000 Faculty Rev), 119
doi: 10.12688/f1000research.7180.1

Cosgrove DJ. 2018. Diffuse growth of plant cell walls. *Plant Physiology* **176**, 16–27.

DeBolt S, Harris D, Stork J. 2013. Plants and plant products useful for biofuel manufacture and feedstock, and methods of producing same. US 8,383,888 B1.

Dick-Pérez M, Zhang Y, Hayes J, Salazar A, Zabotina OA, Hong M. 2011. Structure and interactions of plant cell-wall polysaccharides by two- and three-dimensional magic-angle-spinning solid-state NMR. *Biochemistry* **50**, 989–1000.

Dische Z. 1962. General color reactions. In: Whistler RL, Wolfrom ML, eds. *Methods in carbohydrate chemistry*. New York: Academic Press, 478–481.

Edelmann HG. 1997. Gravistimulated asymmetries in the outer epidermal cell walls of graviresponding coleoptiles. *Planta* **203**(Suppl 1), S123–S129.

Edelmann HG, Samajova O. 1999. Physiological evidence for the accumulation of restrained wall loosening potential on the growth-inhibited side of graviresponding rye coleoptiles. *Plant Biology* **1**, 57–60.

Filisetti-Cozzi TM, Carpita NC. 1991. Measurement of uronic acids without interference from neutral sugars. *Analytical Biochemistry* **197**, 157–162.

Gendreau E, Traas J, Desnos T, Grandjean O, Caboche M, Höfte H. 1997. Cellular basis of hypocotyl growth in *Arabidopsis thaliana*. *Plant Physiology* **114**, 295–305.

Goda H, Shimada Y, Asami T, Fujioka S, Yoshida S. 2002. Microarray analysis of brassinosteroid-regulated genes in *Arabidopsis*. *Plant Physiology* **130**, 1319–1334.

Goubet F, Barton CJ, Mortimer JC, Yu X, Zhang Z, Miles GP, Richens J, Liepman AH, Seffen K, Dupree P. 2009. Cell wall glucomannan in *Arabidopsis* is synthesised by CSLA glycosyltransferases, and influences the progression of embryogenesis. *Plant Journal* **60**, 527–538.

Gupta A, Singh M, Jones AM, Laxmi A. 2012. Hypocotyl directional growth in *Arabidopsis*: a complex trait. *Plant Physiology* **159**, 1463–1476.

Hejnowicz Z. 1997. Graviresponses in herb and trees: a major role for the redistribution of tissue and growth stresses. *Planta* **203**(Suppl 1), S136–S146.

Hosoo Y, Yoshida M, Imai T, Okuyama T. 2002. Diurnal difference in the amount of immunogold-labeled glucomannans detected with field emission scanning electron microscopy at the innermost surface of developing secondary walls of differentiating conifer tracheids. *Planta* **215**, 1006–1012.

Hu L, Mei Z, Zang A, Chen H, Dou X, Jin J, Cai W. 2013. Microarray analyses and comparisons of upper or lower flanks of rice shoot base preceding gravitropic bending. *PLoS One* **8**, e74646.

Huang S, Makarem M, Kiemle SN, Zheng Y, He X, Ye D, Gomez EW, Gomez ED, Cosgrove DJ, Kim SH. 2018. Dehydration-induced physical strains of cellulose microfibrils in plant cell walls. *Carbohydrate Polymers* **197**, 337–348.

Huff J. 2015. The Airyscan detector from ZEISS: confocal imaging with improved signal-to-noise ratio and super-resolution. *Nature Methods* **12**, i–ii.

Ikushima T, Soga K, Hoson T, Shimmen T. 2008. Role of xyloglucan in gravitropic bending of azuki bean epicotyl. *Physiologia Plantarum* **132**, 552–565.

Ivakov A, Flis A, Apelt F, Fünfgeld M, Scherer U, Stitt M, Kragler F, Vissenberg K, Persson S, Suslov D. 2017. Cellulose synthesis and cell expansion are regulated by different mechanisms in growing *Arabidopsis* hypocotyls. *Plant Cell* **29**, 1305–1315.

Joo JH, Bae YS, Lee JS. 2001. Role of auxin-induced reactive oxygen species in root gravitropism. *Plant Physiology* **126**, 1055–1060.

Krieger G, Shkolnik D, Miller G, Fromm H. 2016. Reactive oxygen species tune root tropic responses. *Plant Physiology* **172**, 1209–1220.

Liu X, Yang Q, Wang Y, Wang L, Fu Y, Wang X. 2018. Brassinosteroids regulate pavement cell growth by mediating BIN2-induced microtubule stabilization. *Journal of Experimental Botany* **69**, 1037–1049.

Maris A, Kaewthai N, Eklöf JM, Miller JG, Brumer H, Fry SC, Verbelen J-P, Vissenberg K. 2011. Differences in enzymic properties of five recombinant xyloglucan endotransglucosylase/hydrolase (XTH) proteins of *Arabidopsis thaliana*. *Journal of Experimental Botany* **62**, 261–271.

Millar KD, Kiss JZ. 2013. Analyses of tropistic responses using metabolomics. *American Journal of Botany* **100**, 79–90.

Miller ND, Parks BM, Spalding EP. 2007. Computer-vision analysis of seedling responses to light and gravity. *Plant Journal* **52**, 374–381.

Morita MT. 2010. Directional gravity sensing in gravitropism. *Annual Review of Plant Biology* **61**, 705–720.

Neumetzler L. 2010. *Identification and characterization of Arabidopsis mutants associated with xyloglucan metabolism*. Berlin: Rhombos-Verlag.

Paredes AR, Somerville CR, Ehrhardt DW. 2006. Visualization of cellulose synthase demonstrates functional association with microtubules. *Science* **312**, 1491–1495.

Park YB, Cosgrove DJ. 2012. A revised architecture of primary cell walls based on biomechanical changes induced by substrate-specific endoglucanases. *Plant Physiology* **158**, 1933–1943.

Pelletier S, Van Orden J, Wolf S, et al. 2010. A role for pectin de-methylesterification in a developmentally regulated growth acceleration in dark-grown *Arabidopsis* hypocotyls. *New Phytologist* **188**, 726–739.

- Phyo P, Wang T, Xiao C, Anderson CT, Hong M.** 2017a. Effects of pectin molecular weight changes on the structure, dynamics, and polysaccharide interactions of primary cell walls of *Arabidopsis thaliana*: insights from solid-state NMR. *Biomacromolecules* **18**, 2937–2950.
- Phyo P, Wang T, Kiemle SN, O'Neill H, Pingali SV, Hong M, Cosgrove DJ.** 2017b. Gradients in wall mechanics and polysaccharides along growing inflorescence stems. *Plant Physiology* **175**, 1593–1607.
- Popper ZA.** 2008. Evolution and diversity of green plant cell walls. *Current Opinion in Plant Biology* **11**, 286–292.
- Popper ZA, Tuohy MG.** 2010. Beyond the green: understanding the evolutionary puzzle of plant and algal cell walls. *Plant Physiology* **153**, 373–383.
- Preston RD.** 1982. The case for multinet growth in growing walls of plant cells. *Planta* **155**, 356–363.
- Ray PM, Green PB, Cleland R.** 1972. Role of turgor in plant cell growth. *Nature* **239**, 47–48.
- Refrégier G, Pelletier S, Jaillard D, Höfte H.** 2004. Interaction between wall deposition and cell elongation in dark-grown hypocotyl cells in *Arabidopsis*. *Plant Physiology* **135**, 959–968.
- Roelofsen PA.** 1958. Cell-wall structure as related to surface growth. *Acta Botanica Neerlandica* **7**, 77–89.
- Ryden P, Sugimoto-Shirasu K, Smith AC, Findlay K, Reiter WD, McCann MC.** 2003. Tensile properties of *Arabidopsis* cell walls depend on both a xyloglucan cross-linked microfibrillar network and rhamnogalacturonan II-borate complexes. *Plant Physiology* **132**, 1033–1040.
- Sánchez-Rodríguez C, Bauer S, Hématy K, et al.** 2012. Chitinase-like1/pom-pom1 and its homolog CTL2 are glucan-interacting proteins important for cellulose biosynthesis in *Arabidopsis*. *Plant Cell* **24**, 589–607.
- Sánchez-Rodríguez C, Ketelaar K, Schneider R, Villalobos JA, Somerville CR, Persson S, Wallace IS.** 2017. BRASSINOSTEROID INSENSITIVE2 negatively regulates cellulose synthesis in *Arabidopsis* by phosphorylating cellulose synthase 1. *Proceedings of the National Academy of Sciences USA* **114**, 3533–3538.
- Sawake S, Tajima N, Mortimer JC et al.** 2015. KONJAC1 and 2 are key factors for GDP-mannose generation and affect L-ascorbic acid and glucomannan biosynthesis in *Arabidopsis*. *Plant Cell* **27**, 3397–3409.
- Schröder R, Atkinson RG, Redgwell RJ.** 2009. Re-interpreting the role of endo-beta-mannanases as mannan endotransglycosylase/hydrolases in the plant cell wall. *Annals of Botany* **104**, 197–204.
- Selvendran RR, O'Neill MA.** 1987. Isolation and analysis of cell walls from plant material. *Methods of Biochemical Analysis* **32**, 25–153.

Shah DU, Reynolds TPS, Ramage MH. 2017. The strength of plants: theory and experimental methods to measure the mechanical properties of stems. *Journal of Experimental Botany* **68**, 4497–4516.

Shinohara N, Sunagawa N, Tamura S, Yokoyama R, Ueda M, Igarashi K, Nishitani K. 2017. The plant cell-wall enzyme AtXTH3 catalyses covalent cross-linking between cellulose and cello-oligosaccharide. *Scientific Reports* **7**, 46099.

Singh AP, Savaldi-Goldstein S. 2015. Growth control: brassinosteroid activity gets context. *Journal of Experimental Botany* **66**, 1123–1132.

Singh KL, Mukherjee A, Kar RK. 2017. Early axis growth during seed germination is gravitropic and mediated by ROS and calcium. *Journal of Plant Physiology* **216**, 181–187.

Song L, Zhou XY, Li L, Xue LJ, Yang X, Xue HW. 2009. Genome-wide analysis revealed the complex regulatory network of brassinosteroid effects in photomorphogenesis. *Molecular Plant* **2**, 755–772.

Sørensen I, Domozych D, Willats WG. 2010. How have plant cell walls evolved? *Plant Physiology* **153**, 366–372.

Sun Y, Fan XY, Cao DM, et al. 2010. Integration of brassinosteroid signal transduction with the transcription network for plant growth regulation in *Arabidopsis*. *Developmental Cell* **19**, 765–777.

Suslov D, Verbelen JP. 2006. Cellulose orientation determines mechanical anisotropy in onion epidermis cell walls. *Journal of Experimental Botany* **57**, 2183–2192.

Suslov D, Verbelen JP, Vissenberg K. 2009. Onion epidermis as a new model to study the control of growth anisotropy in higher plants. *Journal of Experimental Botany* **60**, 4175–4187.

Tan L, Eberhard S, Pattathil S, et al. 2013. An *Arabidopsis* cell wall proteoglycan consists of pectin and arabinoxylan covalently linked to an arabinogalactan protein. *Plant Cell* **25**, 270–287.

Vandenbussche F, Petrásek J, Zádňíková P, et al. 2010. The auxin influx carriers AUX1 and LAX3 are involved in auxin-ethylene interactions during apical hook development in *Arabidopsis thaliana* seedlings. *Development* **137**, 597–606.

Vandenbussche F, Suslov D, De Grauwe L, Leroux O, Vissenberg K, Van der Straeten D. 2011. The role of brassinosteroids in shoot gravitropism. *Plant Physiology* **156**, 1331–1336.

Vilím V. 1985. Colorimetric estimation of uronic acids using 2-hydroxydiphenyl as a reagent. *Biomedica Biochimica Acta* **44**, 1717–1720.

Whitney SEC, Brigham JE, Darke AH, Reid JSG, Gidley MJ. 1998. Structural aspects of the interaction of mannanbased polysaccharides with bacterial cellulose. *Carbohydrate Research* **307**, 299–309.

Wickett NJ, Mirarab S, Nguyen N, et al. 2014. Phylotranscriptomic analysis of the origin and early diversification of land plants. *Proceedings of the National Academy of Sciences USA* **111**, E4859–E4868.

Xie L, Yang C, Wang X. 2011. Brassinosteroids can regulate cellulose biosynthesis by controlling the expression of *CESA* genes in *Arabidopsis*. *Journal of Experimental Botany* **62**, 4495–4506.

Yu X, Li L, Zola J, et al. 2011. A brassinosteroid transcriptional network revealed by genome-wide identification of BES1 target genes in *Arabidopsis thaliana*. *Plant Journal* **65**, 634–646.

Zhang Q, Pettolino FA, Dhugga KS, et al. 2011. Cell wall modifications in maize pulvini in response to gravitational stress. *Plant Physiology* **156**, 2155–2171.

Zhang T, Vavylonis D, Durachko DM, Cosgrove DJ. 2017. Nanoscale movements of cellulose microfibrils in primary cell walls. *Nature Plants* **3**, 17056.

Zhou L, Hou H, Yang T, Lian Y, Sun Y, Bian Z, Wang C. 2018. Exogenous hydrogen peroxide inhibits primary root gravitropism by regulating auxin distribution during *Arabidopsis* seed germination. *Plant Physiology and Biochemistry* **128**, 126–133.

Table 1. Overview of cellulose microfibril orientations

Treatment	Cellulose orientation ^a				Number of repeats
	transverse	oblique	random	longitudinal	
Col-0, upper	1.82±0.70	0.09±0.28	0.08±0.25	1.43±0.63	38
Col-0, lower	1.18±0.56	0.16±0.37	0.05±0.27	1.89±0.51	38
Col-0+EBL, upper	0.42±0.69	0.47±0.77	0.10±0.30	1.53±0.61	19
Col-0+EBL, lower	0.33±0.55	1.40±0.72	0.43±0.63	0.63±0.56	30
Col-0+BRZ, upper	1.48±0.60	0.02±0.09	0.26±0.44	1.82±0.67	31
Col-0+BRZ, lower	0.65±0.49	0.09±0.29	0.17±0.39	1.91±0.29	23
Col-0+ory, upper	0.90±0.84	0.52±0.70	1.22±0.85	1.56±0.73	25
Col-0+ory, lower	0.23±0.44	0.15±0.38	0.77±0.60	2.00±0.00	13
Col-0+ory+BRZ, upper	0.63±0.66	0.22±0.36	1.13±0.67	1.32±0.75	26
Col-0+ory+BRZ, lower	0.20±0.41	0.11±0.32	1.20±0.70	1.90±0.31	20

^a Cellulose microfibril orientation across the whole thickness of outer epidermal cell walls was determined using S4B dye, spinning-disc and super-resolution confocal microscopy. The prevalence of each type of cellulose microfibril orientation in every Z-stack was characterized by scores 1 to 3 as high (3), intermediate (2) or low (1). Then these values were averaged between all Z-stacks for a given treatment and presented as means ± SD.

Table 2. *Stimulation of gravitropic bending by brassinazole is impaired in the triple csla2csla3csla9 mutant compared with Col-0 plants*

Comparison	Time after gravistimulation, hours											
	1	2	3	4	5	6	7	8	9	10	11	12
	<i>Stimulation of bending, fold^a</i>											
<i>Col-0</i> + BRZ vs. <i>Col-0</i>	12.8	13.0	12.4	6.4	3.2	2.5	2.4	1.9	2.0	1.8	1.9	2.0
<i>csla2csla3csla9</i> + BRZ vs. <i>csla2csla3csla9</i>	5.0	4.6	3.2	3.1	2.6	1.8	1.8	1.7	1.7	1.4	1.7	1.5

^a Gravitropic bending in the presence of BRZ (Fig. 6) was divided by that without BRZ for *Col-0* and *csla2csla3csla9*, respectively.

Figure legends

Fig. 1. Brassinosteroids affect gravitropism of hypocotyls in Arabidopsis plants. Etiolated *Col-0* seedlings were grown on horizontal Petri plates with one-half strength agarized Murashige and Skoog medium without supplements (A), with 100 nM EBL (B) or 1 μ M BRZ (C). Five-day-old plants were photographed.

Fig. 2. Brassinosteroids change cell wall mechanics in Arabidopsis hypocotyls. (A) The schematic representation of regions extended by the creep method (orange shadings) in hypocotyls of different age. Arrowheads mark borders of growing zones in hypocotyls of *Col-0* plants of the respective age. Changes in creep rates by BRZ (1 μ M) in hypocotyls of 6-day-old *Col-0* plants (B) and by EBL (100 nM) in hypocotyls of 3-day-old (C), 5-day-old (D) and 6-day-old (E) *Col-0* plants. Creep rates were measured under 750 mg (B, C, E) or 625 mg (D) loads. Data are means \pm SE (n=10). Different letters in (B) mark significant differences ($P < 0.05$) revealed by Games-Howell's post-hoc test performed after ANOVA. Asterisks in (C-E) denote significant difference ($*P < 0.05$; $**P < 0.01$) between the respective zones of EBL-grown and control seedlings determined by Student's *t*-test.

Fig. 3. Biochemical composition of cell walls in Arabidopsis plants as affected by brassinosteroids. The levels of uronic acids (A), crystalline cellulose (B) and the monosaccharide composition of cell wall matrix polymers (C) were determined in 5-day-old etiolated *Col-0* seedlings without supplements in the growth medium (control), in the presence of 1 μ M BRZ or 100 nM EBL. Data are means \pm SE (n=9). Asterisks denote significant differences ($*P < 0.05$; $**P < 0.01$) revealed by Dunnett's post-hoc test performed after ANOVA.

Fig. 4. Brassinosteroid and oryzalin effects on the arrangement of cellulose macrofibrils in the outer epidermal cell wall of hypocotyls from 5-day-old etiolated *Col-0* Arabidopsis plants. Hypocotyls were extracted under mild conditions and their walls were stained with Pontamine Fast Scarlet 4B, the cellulose-specific fluorescent dye. Cellulose orientation is shown (A) in the upper growing and (D) the lower non-growing region of hypocotyls from control seedlings grown on one-half strength agarized Murashige and Skoog medium without supplements; (B) the upper and (E) the lower region of hypocotyls from plants grown in the presence of 100 nM EBL; (C) the upper and (F) the lower region of hypocotyls from plants grown in the presence of 1 μ M BRZ; (G) the upper and (I) the lower

region of hypocotyls from plants grown in the presence of 250 nM oryzalin; (H) the upper and (J) the lower region of hypocotyls from plants grown in the presence of 1 μ M BRZ and 250 nM oryzalin.

Fig. 5. Cellulose orientation affects the percentage of standing *Arabidopsis* hypocotyls. Col-0 seedlings were grown in darkness on horizontal Petri plates for 5 days without supplements (white bar), with 250 nM oryzalin (orange bar), in each case with 1 μ M BRZ (hatched bars) or without (solid color bars). Data are means \pm SE (n=6). Different letters denote the significant difference between control and oryzalin-grown plants ($P=0.0017$; Student's *t*-test). Asterisks indicate significant effects of BRZ in control or oryzalin-grown seedlings (** $P < 0.01$; *** $P < 0.001$; Student's *t*-test).

Fig. 6. Elimination of glucomannans in the triple *cs/a2cs/a3cs/a9* mutant plants increases gravitropic bending of hypocotyls. Etiolated Col-0 and *cs/a2cs/a3cs/a9* mutant seedlings were grown on vertical Petri plates with or without 1 μ M BRZ for 3 days, subsequently gravistimulated by a 90-degree clockwise rotation of the plates, and gravitropic bending of their hypocotyls was followed by an infrared imaging system for 12 h. Data are means \pm SE (n=10). Asterisks denote significant differences (* $P < 0.05$; ** $P < 0.01$; Student's *t*-test) between *cs/a2cs/a3cs/a9* and Col-0 plants.

Fig. 7. BRZ inhibits cell expansive growth at the base of *Arabidopsis* hypocotyls. (A) Epidermal cell length distribution along the lower parts of hypocotyls in 55- and 72-hour-old etiolated Col-0 seedlings grown with 1 μ M BRZ or without (control). Cells are numbered from the base of hypocotyls towards cotyledons. Data are means \pm SE (n=9). All the cells are significantly shorter in the presence of BRZ than the respective control cells ($P < 0.01$; Student's *t*-test) with the exception of cells 1 in 55-hour-old plants (not shown on the plot A). (B) Average cell expansion rates at the base of hypocotyls calculated from the data of plot A (means \pm SE, n=9). Asterisks mark significant differences (* $P < 0.05$; ** $P < 0.01$; *** $P < 0.001$; Student's *t*-test).

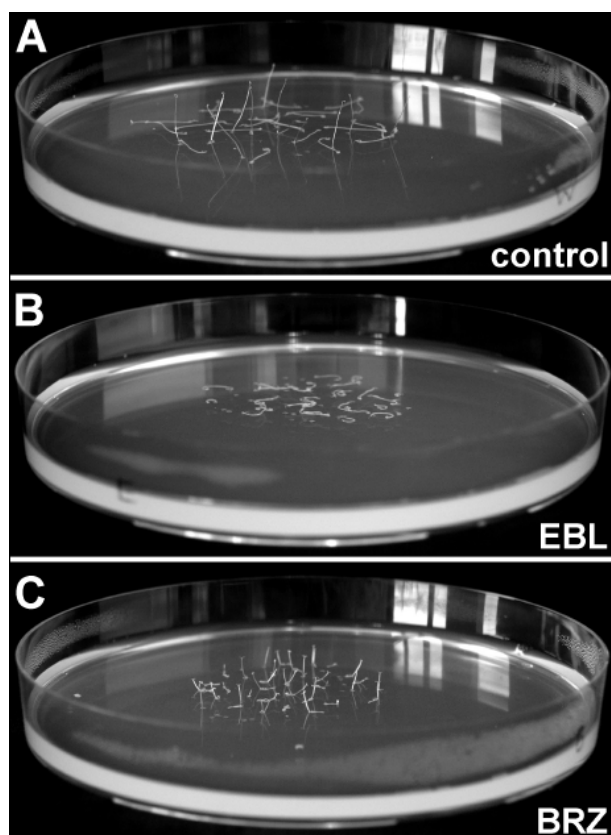


Fig. 1.

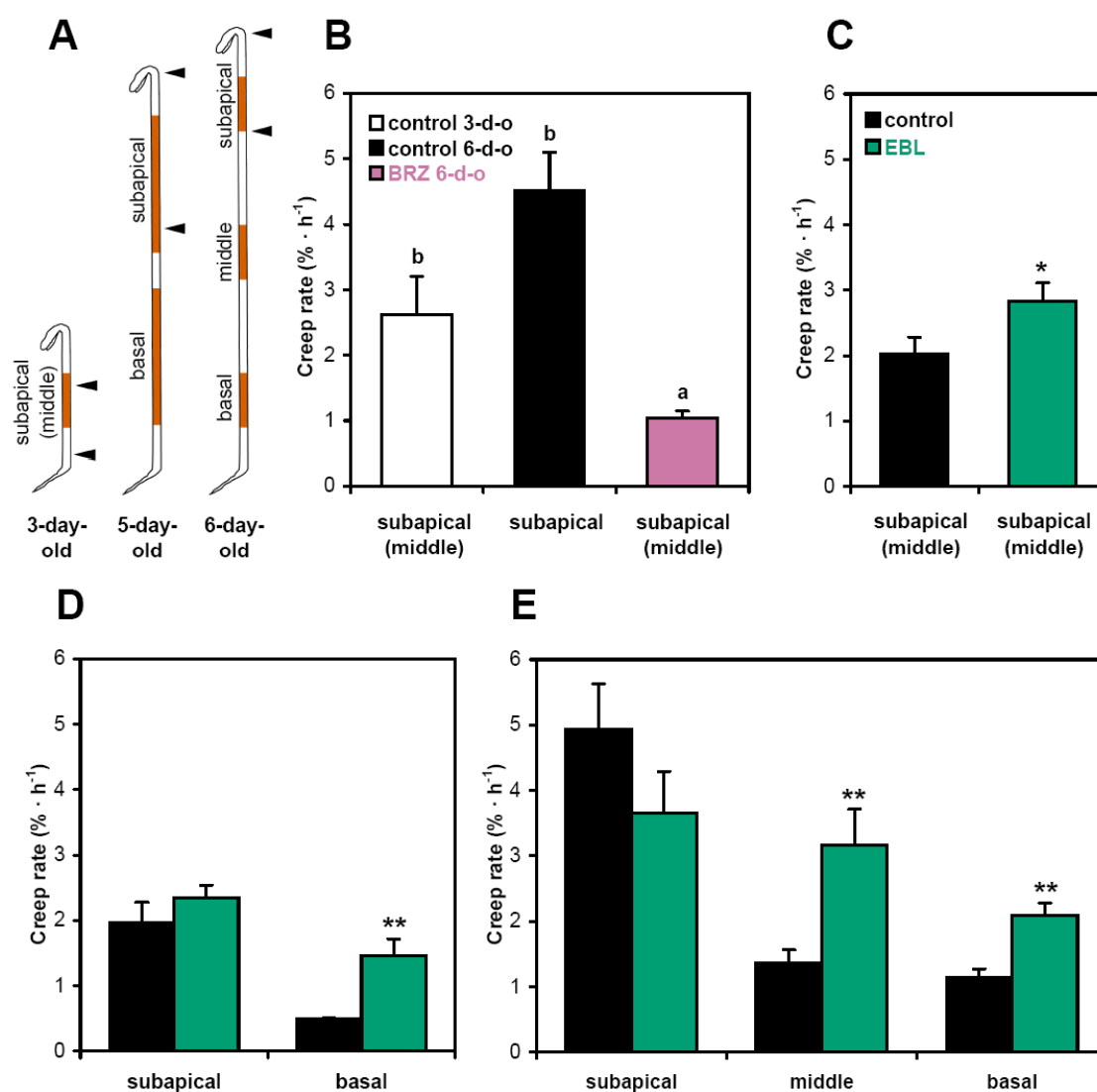


Fig. 2.

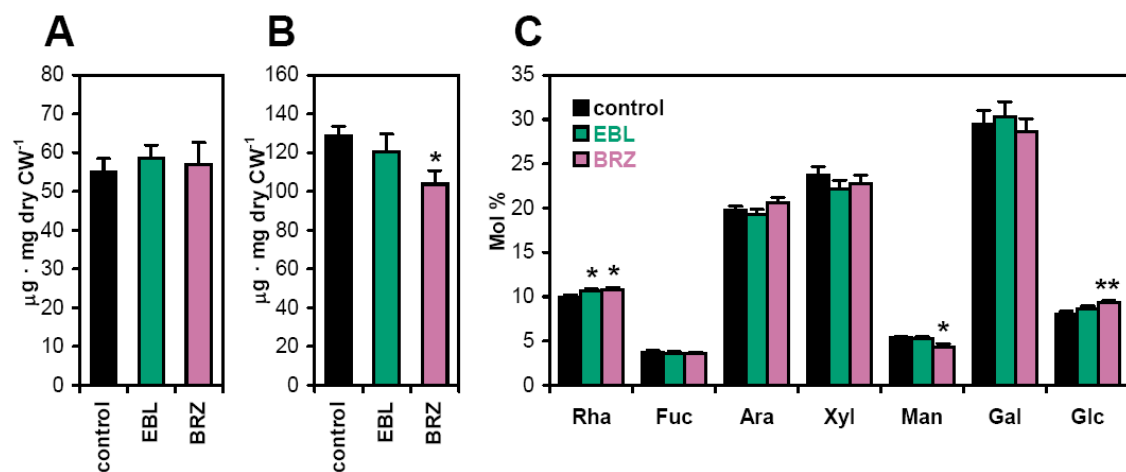


Fig. 3.

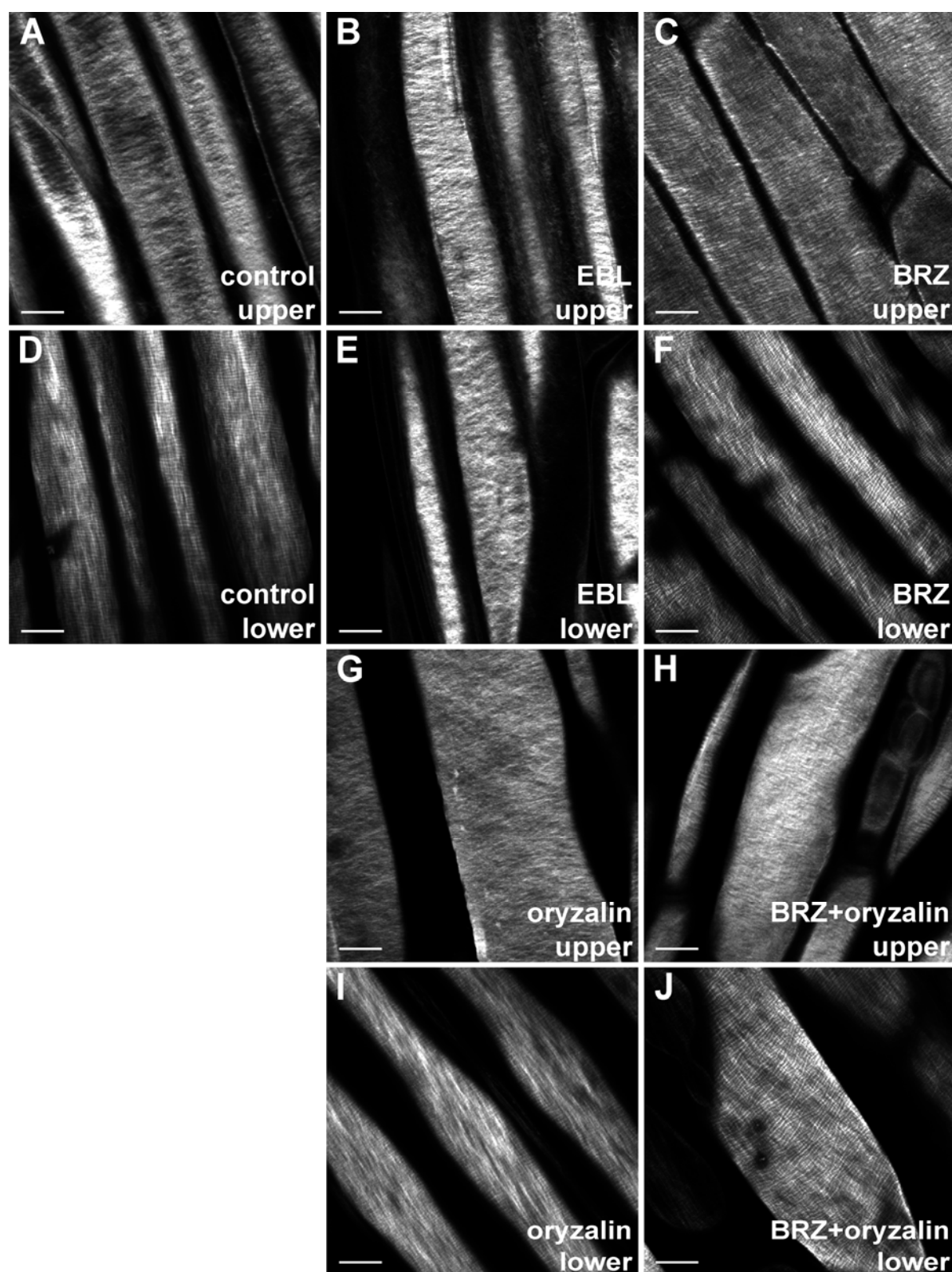


Fig. 4.

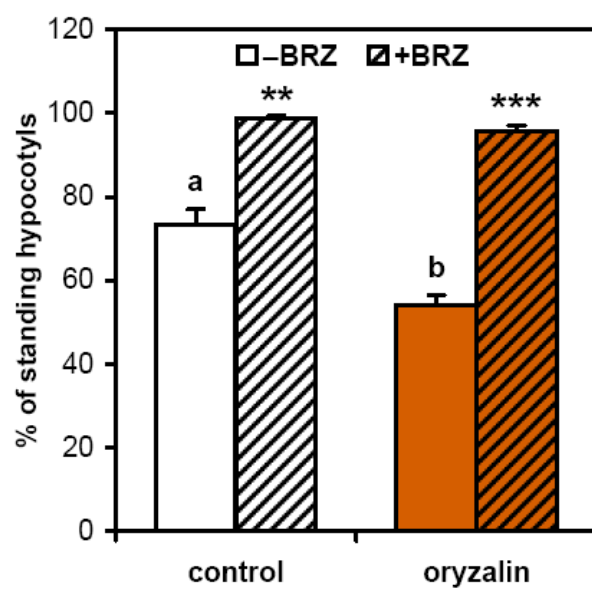


Fig. 5.

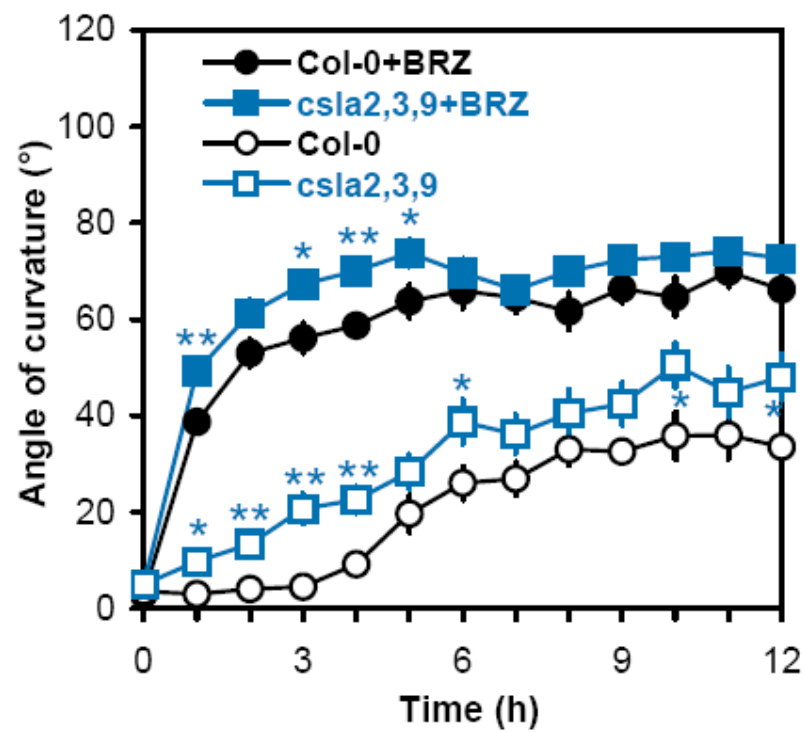


Fig. 6.

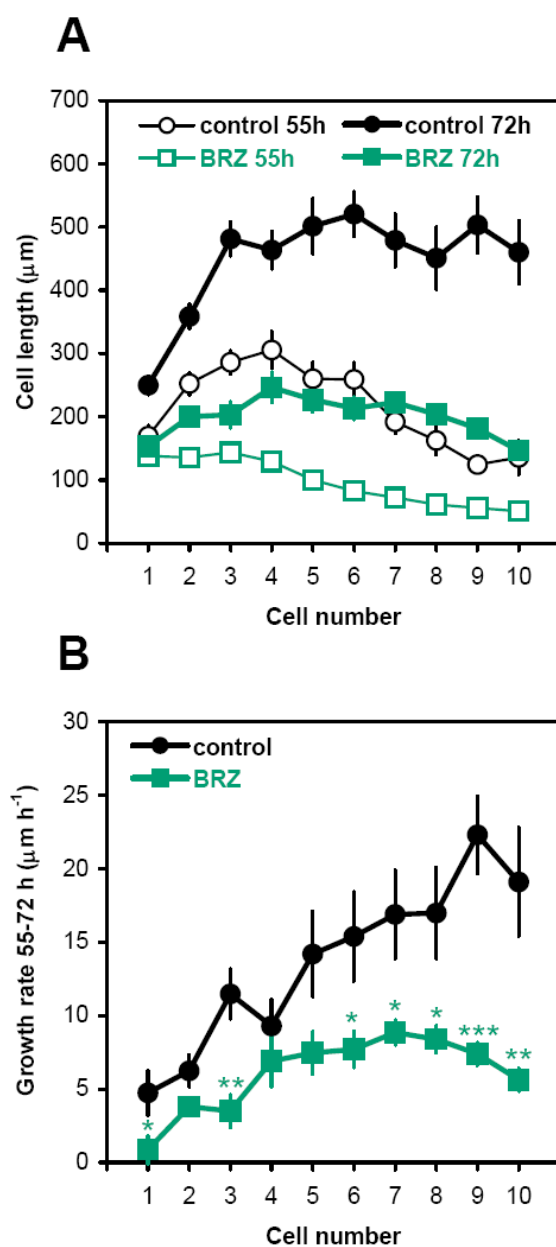


Fig. 7.